Journal of Robotics and Control (JRC)
Volume 5, Issue 6, 2024
ISSN: 2715-5072, DOI: 10.18196/jrc.v5i6.23867

Application of Terminal Synergetic Control Based Water Strider Optimizer for Magnetic Bearing Systems

Mina Q. Kadhim [1], Farazdaq R. Yaseen [2], Huthaifa Al-Khazraji [3*], Amjad J. Humaidi [4]
[1, 2, 3, 4] Control and System Engineering Department, University of Technology- Iraq
Email: [1] Mina.q.kadhim@uotechnology.edu.iq, [2] 60002@uotechnology.edu.iq, [3] 60141@uotechnology.edu.iq,
[4] amjad.j.humaidi@uotechnology.edu.iq
*Corresponding Author

***Abstract*—Magnetic bearing (Magb) system is a modern and future electromagnetic device that has many advantages and applications. The open-loop dynamics of the Magb system has a nonlinear and unusable characteristic. In the present paper, a novel robust and advance terminal synergetic control (TSC) approach is developed to stabilize position of the Magb system. The controller is design based on the Magb model using the synergetic control associated with the terminal attractor method. The proposed control algorithm has the advantage of developing a control law which is continuous, chattering free, and allows for a more rapid system response. For further enhancement of the controller performance, a population-based algorithm named water strider optimizer (WSO) has been utilized to adjust the tunable coefficients of the control algorithm. In order to approve the ability and the performance of the proposed control approach, a simulation comparison results with the classic synergetic control (CSC) is conducted. Based on the simulation results, the TSC improves the settling time by 50% and the ITAE index by 45.3% as compared to the CSC. In addition, the recovery time under an external disturbance has been improved by 50% as compared to the CSC. These outcomes demonstrate that the proposed control algorithm allows for rapidly in the system response and more robustness.**

Keywords—Magnetic Bearing; Nonlinear Control; Robust Control; Terminal Synergetic Control; Swarm Optimization; Water Strider Optimizer.

I. INTRODUCTION

The magnetic bearing (Magb) system is an electromagnetic device which is regulated by electromagnetic energy to levitate a rotating part without the need for physical contact with the stator part [1]. Magb systems provide significant benefits over conventional bearings because they have no contact with the rotor, including reduced heat losses, vibration isolation, no lubrication, reduced friction, and noiseless operation [2]-[4]. As a result, Magb has been extensively employed in numerous industrial applications, including vacuum pumps, turbines, high-speed motors, and wheel energy storage [5]. Due to the inherently unstable nature of Magb system, feedback control is critical for levitation. With the continuous development of controllers, many classical and advanced control algorithms have been applied to the Magb system.

For its easy implementation, the proportional-integral-derivative (PID) controller was employed by Psonis et al. [4] and Gupta et al. [6] for controlling the Magb system. To enhance the performance of the PID controller, Yixin et al. [7] and Bo et al. [5], introduced fuzzy-PID controller to manipulate the Magb system. Du et al. [8] optimized the parameters of the PID controller by reformative artificial bee colony (RABC) which is an improved version of the original ABC. An extensive comparison of different control structures including linear-quadratic (LQ), LQ with loop transfer recovery (LTR), PID and PI-PD controllers applied to the Magb system are presented by Jastrzębski and Pöllänen [9]. The tuning of the adjustable coefficients of the controllers was performed via on the genetic algorithm (GA). The outcomes of the study show that PID and LQ control methods achieved similar results. With the LTR, LQ-LTR provides better performance and robustness. A modified version of the PID, fractional order PID (FOPID), was adopted by Chang and Chen [10]. An adaptive genetic algorithm (AGA) was used to optimize the FOPID controller. The second-order SMC (sliding mode control) combined with ADRC (active disturbance rejection control) were used by Wang et al. [1] and Yu et al. [11] respectively to improve the efficiency of the Magb system. Al-Khazraji et al. [12] examined the performance of the SMC and backstepping control (BSC) for Magb systems. The simulation results indicated a superior performance and strong disturbance rejection of the SMC in comparison with the BSC.

The desirable property of the nonlinear synergetic control (SC) seems to be a new effective approach to deal with numerous control problems [13]-[15]. Besides, terminal technique was introduced for more attractive performance which is makes the tracking error converge to zero in finite time [16]. Therefore, in this paper, the terminal synergetic control (TSC) algorithm is developed to regulate position of the Magb system. In addition, exploring the performance of combining the design of the TSC with new development swarm optimization techniques is also investigated. In this context, a water strider optimizer (WSO) has been introduced. The main idea of using the WSO is to find best selection of the design variables of the TSC for further improvement of the Magb system.

II. MATHEMATICAL MODEL

The magnetic bearing (Magb) system consists of a levitated rotor, electromagnetic coil and stator core [1]. For the purpose of controller design, the Magb system is modeled as a one-degree-of-freedom in the Y-direction as shown in Fig. 1. The mathematical model of the Magb system shapes the relationship between the magnetic force, displacement and current [11]-[12].

The electromagnetic attractive force (F_m) is defined according to the Maxwell's formula as:

$$F_m = \frac{\beta^2 A}{\mu_0} \tag{1}$$

where β is the intensity of the magnetic induction that is generated by the stator and the rotor which is defined in Eq. (2), A is the section area, μ_0 is the vacuum permeability.

$$\beta = \frac{\mu_0 NI}{\delta_0} \tag{2}$$

where N is number of coil turns, I is the current and δ_0 is air gap. Substituting Eq. (2) into Eq. (1), the result is:

$$F_m = k\frac{I^2}{{\delta_0}^2} \tag{3}$$

where $k = \mu_0 N^2 A$.

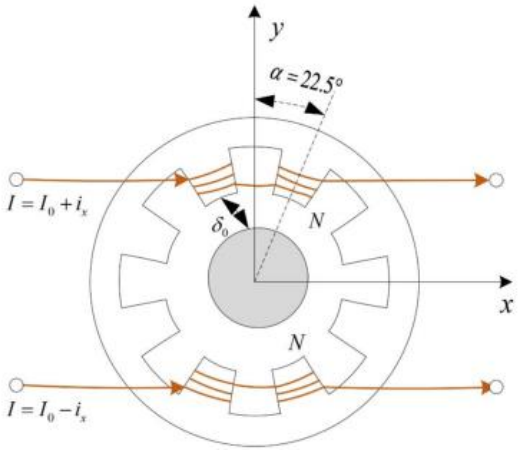

Fig. 1. Magb system

There are two attraction forces acting on the levitated rotor. These two attraction forces are the upper attraction force (F_{mu}) as given in Eq. (4) and lower attraction forces (F_{ml}) as given in Eq. (5) [11].

$$F_{mu} = \frac{1}{2}k\frac{(I_0 - i)^2}{(\delta_0 + x\cos\alpha)^2} \tag{4}$$

$$F_{ml} = \frac{1}{2}k\frac{(I_0 + i)^2}{(\delta_0 - x\cos\alpha)^2} \tag{5}$$

where α stands for the angle formed by stator's central axis and the electromagnet's center line, x is the displacement of the rotor and i is the control input current. The resultant attractive electromagnetic force (F_{mt}) in direction of the Y-axis is given by the difference between F_{ml} and F_{mu} as follows:

$$F_{mt} = 2F_{ml}\cos\alpha - 2F_{mu}\cos\alpha \tag{6}$$

By substitute Eq. (4) and (5) into Eq. (6), the result is:

$$F_{mt} = k\cos\alpha\left(\frac{(I_0 + i)^2}{(\delta_0 - x\cos\alpha)^2} - \frac{(I_0 - i)^2}{(\delta_0 + x\cos\alpha)^2}\right) \tag{7}$$

At $x = 0, i = I_0$, the equilibrium point, by using Taylor expansion for Eq. (7), Eq. (8) can be obtained after removing the higher order with small amplitude quantities.

$$F_{mt} = k_x x + k_i i \tag{8}$$

where $k_x = 4\mu_0 N^2 A\cos\alpha\frac{{I_0}^2}{{\delta_0}^2}$ is displacement stiffness coefficient and $k_i = 4\mu_0 N^2 A\cos\alpha\frac{I_0}{{\delta_0}^2}$ is current stiffness coefficient.

By using the 2nd Newton's law of motion, the equation that represented the motion of the rotor with respect to the electromagnetic force action is formulated by:

$$m\ddot{x} = F_{mt} \tag{9}$$

Using the result of Eq. (8) into Eq. (9) yield:

$$m\ddot{x} = k_x x + k_i i \tag{10}$$

Let x_1, x_2 and u stand for the position x, the velocity $\dot{x}$ and the control input i. Then, the Magb system is modeled mathematically as follows:

$$\dot{x}_1 = x_2 \tag{11}$$

$$\dot{x}_2 = \frac{k_x}{m}x_1 + \frac{k_i}{m}u \tag{12}$$

III. CONTROLLER DESING

Feedback control algorithms have the ability to adjust the dynamics of the systems to the predefined performance [17]-[19]. Over the years, many types of control systems have been introduced to cover a wide range of systems [20]-[22]. SC technique has been widely used to control numerous systems. In this section, the procedure to design the classical SC (CSC) and Terminal SC (TSC) for the Magb system is presented. One of the advantages of designing the CSC and the TSC is that they do not require the linearization of the Magb system. For the purpose of designing CSC and TSC, Eq. (11) can be revised as follows:

$$\dot{x}_2 = f_x + bu \tag{13}$$

where $f_x = \frac{k_x}{m}x_1$ and $b = \frac{k_i}{m}$

Let define the tracking error e_t as the difference between the desired position x_{1d} and the actual position x_1 as follows:

$$e_t = x_{1d} - x_1 \tag{14}$$

The results of taking the 1st and the 2nd time derivatives of e_t are given in Eq. (15) and (16):

$$\dot{e}_t = \dot{x}_{1d} - \dot{x}_1 = \dot{x}_{1d} - x_2 \tag{15}$$

$$\ddot{e}_t = \ddot{x}_{1d} - \dot{x}_2 \tag{16}$$

In CSC method, the marco-variable φ is defined as (17).

$$\varphi = \dot{e}_t + c_1 e_t \quad (17)$$

where $c_1 (c_1 > 0)$ is a scalar designing parameter.

Taking the 1st derivative of the φ gives:

$$\dot{\varphi} = \ddot{e}_t + c_1 \dot{e}_t \quad (18)$$

The motion of the synthesized system must satisfy the following system of functional equations:

$$\dot{\varphi} + c_2 \varphi = 0 \quad (19)$$

where $c_2 (c_2 > 0)$ is a scalar designing parameter.

Substitute Eq. (16) in Eq. (19) gives:

$$\ddot{x}_{1d} - f(x) - g(x)u + c_2 \dot{e}_t + c_2 \varphi = 0 \quad (20)$$

Solving for u gives:

$$u_{CSC} = \frac{1}{b}(-f_x + c_1 \dot{e}_t + c_2 \varphi) \quad (21)$$

In terms of TSC, the marco-variable φ is defined as follows:

$$\varphi = c_1 e^{\frac{q}{p}} + \dot{e} \quad (22)$$

where $p > q > 0$.

Take the first derivative of φ gives:

$$\dot{\varphi} = \frac{c_1 q}{p}\left(e^{1-\frac{q}{p}}\right)\dot{e} + \ddot{e} \quad (23)$$

Select state trajectories of φ as:

$$\dot{\varphi} + c_2 \varphi = 0 \quad (24)$$

Substitute $\dot{\varphi}$ gives:

$$\frac{c_1 q}{p}\left(e^{1-\frac{q}{p}}\right) + \ddot{e} + c_2 \varphi = 0 \quad (25)$$

Substitute $\ddot{e}$:

$$\frac{c_1 q}{p}\left(e^{1-\frac{q}{p}}\right)\dot{e} - f_x - bu + c_2 \varphi = 0 \quad (26)$$

Solving for u:

$$u_{TSC} = \frac{1}{b}\left(-f_x + \frac{c_1 q}{p}\left(e^{1-\frac{q}{p}}\right)\dot{e} + c_2 \varphi\right) \quad (27)$$

IV. WATER STRIDER OPTIMIZER

The purpose of the optimization is to define the best decision parameters in order to maximize or minimize an objective function. Because of its simplicity and flexibility, and motivated by the social living and hunting of numerous animals, numerous new swarm algorithms were successfully developed and used by the researchers for solving complex problems [24]-[36]. Due to the effectiveness of employing swarm algorithms instead of classical try and error approach, numerous authors utilized swarm optimizations to determine the optimal design parameters of the controller [37]-[46].

The water strider optimizer (WSA) is a swarm-based algorithm that simulates the water strider bug's succession of behaviors including mating style, intelligent ripple communication, territorial behavior, and feeding mechanism [47]. Humans have been fascinated by their amazing ability to live above the water's surface for a considerable amount of time [48]. In fact, they were able to remain above the surface film by employing both hydrophobic legs and surface tension. Other distinctive features of these insects include their behavioral syndromes, communication mechanisms, and modes of locomotion [49]. As shown in Fig. 2, water striders communicate by sending out ripples that carry different kinds of information. Prey and potential predators are also identified using this system [50]. For growth and energy restoration, water striders consume a variety of foods. They consume, for example, tadpoles, planets, spiders, floating-hatched larvae, dead insects, and other protein sources. The water striders can detect ripple signals and seize the land-dwelling insect when it falls into the water and fights for its life [51].

There are five stages in mathematical model of the WSO algorithm starts from the birth, then territory establishment, mating, feeding, and ending with the death. Algorithm 1 presents the pseudo-code that describes the steps of the WSA. In the birth stage, the WSs are initialized randomly within the search space as illustrated in Eq. (28).

$$WS_i^0 = Lb + rand.(Ub - Lb);\ i = 1, 2, \dots, N_{pop} \quad (28)$$

where WS_i^0 denotes the ith WS starting positions in the lake (search space). The terms Lb and Ub stand for the variable's lower and upper bounds, respectively. The population size, or WSs, is represented by N_{pop}, and the random number, $rand$, is between 0 and 1. An objective function assesses the starting positions of WSs in order to determine their fitness.

Fig. 2. Communication between two water striders

WSA generated different territories for the purpose of living, mating, and feeding where n_t is the number of territories. WSA sorts the agents into groups according to their fitness. Each group $\left(\frac{N_{pop}}{nt}\right)$ of WS member is allocated to the j-th territory, where the index $j = 1, 2, \dots, n_t$. The positions of the best and worst cost function in each territory are regarded as the female (optimal foraging-ha-bitat) and male (keystone) positions, respectively. In other words, the females are used to determine the best location of each territory find the food.

Water striders have an amazing process during their mating season. The female responds to the keystone's

courtship calling signals with either attractive or repulsive ripples. There is a p% chance of sending an attraction response, the probability of sending a repulsive response is (1 − p). For the sake of simplicity, it can be assumed p to be 50% since the response from females is unknown. They will approach and mate if the female gives off an attraction signal. In the event that the keystone mates or is repelled, Eq. (29) will determine the keystone's new location.

Algorithm 1. Pseudo-code of the WSA

Inputs:
population size N_{pop}, number of territories, $n_t$the number of iterations T_{max}
Initialization
Initialize the population randomly as given in Eq. (28)
Evaluate the population
Loop:
while $t < T_{max}$do
  Establish n_t and allocate the WSs
  For (each territory) do
    Update the position of the WSs based on Eq. (29)
    Evaluate the new position
    If (no improvement in the objective function is found) **then**
      Update the position of the WSs based on Eq. (31)
      Evaluate the new position
    If (no improvement in the objective function is found) **then**
      Update the position of the WSs based on Eq. (32)
      Evaluate the new position
    End
  End
End
Return WS_{best}

$$WS_i^{t+1} = \begin{cases} WS_i^t + R.rand, & if\ mating\ happens \\ WS_i^t + R.(1 + rand), & otherwise \end{cases} \quad (29)$$

where WS_i^t represents the i-th WS position in the t-th cycle; rand is a random value ranging from 0 and 1; R is a vector of mate's position WS_i^{t+1} in the same territory and its endpoint is at the position of a female WS_F^{t+1}. The selection mechanism of R is proportionate to fitness, like roulette wheel selection, can be used to choose this female [52]. The radius of the ripple wave, or female WSs (WS_F^{t-1}), and male (WS_i^{t-1}) are equal to the length of R, according to Eq. (30).

$$R = WS_F^{t-1} - WS_i^{t-1} \quad (30)$$

The mating process is energy-intensive regardless of whether it is successful or not. Consequently, WSs in the new role forage for food supplies. In order to achieve this, Eq. (31) is defined for moving to the new location around the lake's best WS (WS_{BL}^t), which contains a significant amount of food resources.

$$WS_i^{t+1} = WS_i^t + 2rand(WS_{BL}^t - WS_i^t) \quad (31)$$

The objective function is assessed and contrasted with that of the previous position to ascertain the outcome of the food attainment process. The WS will perish if its new fitness is lower because it will not only be unable to find food but also face a higher risk of combat with other WSs in the destination territory. In this scenario, the recently developed larva will take the place of the deceased WS as the keystone, and his position within the territory is randomly initialized as per Eq. (32). Should things be different, the keystone would still be alive.

$$WS_i^{t+1} = Lb_j^t + 2rand\left(Ub_j^t - Lb_j^t\right) \quad (32)$$

The highest and lowest values of WS's position within jth territory are indicated by the symbols Ub_j^t and Lb_j^t. Stated differently, they establish the limits of deceased WS's domain.

The algorithm stops at maximum number of life cycles (T_{max}) and reports the position with the most experience.

V. SIMULATION RESULTS

The simulation experiments are coded in the m-file of the MATLAB software. The model of the Magb system which is given by Eq. (10) and (11) are utilized to capture the dynamics of the Magb system. To evaluate the performance of the TSC, two scenarios (without/with external disturbance) were considered. The main parameters of the Magb system are reported in Table I [5]. The initial state of Magb system in terms of the rotor's position and velocity is set to -0.03 m and 0 m/s repectivly. The desired position of the rotor is 0 m.

TABLE I. PARAMETERS OF MAGB SYSTEM

Parameters	Values
Current stiffness (k_i)	184.3 N/A
Displacement stiffness (k_x)	1.536×10^6 N/m

To optimize the performance proposed controllers, the WSA is used to tune the design parameters of the controllers. To see the impact of the terminal attractor technique, the tuning parameters (c_1 and c_2) of the CSC is firstly optimized. The same value obtained for the CSC is used in the TSC. Further, the additional adjustable parameters (p and q) are optimized. The objective function of the WSA to tune the performance of the two controllers is determined by the ITAE (Integral Time of Absolute Errors) index as presented in Eq. (33) [53].

$$ITAE = \int_{tt=0}^{tt=t_{sim}} tt|e(t)|dt \quad (33)$$

where t_{sim} is the time of the simulation. The population size (N) of the WSA is 20 and the number of Iterations (T_{max}) is 30.

A. Scenario One: Without Disturbance

In this scenario, a step input is used to evaluate the performance of the TSC. The convergence to the cost function of the WSA is shown in Fig. 3. The settings of the CSC and TSC are listed in Table II.

TABLE II. OPTIMAL SETTING OF CONTROLLER'S DESIGN PARAMETERS

Parameters	Controller	
	CSC	TSC
c_1	10	10
c_2	50	50
p	-	4.5

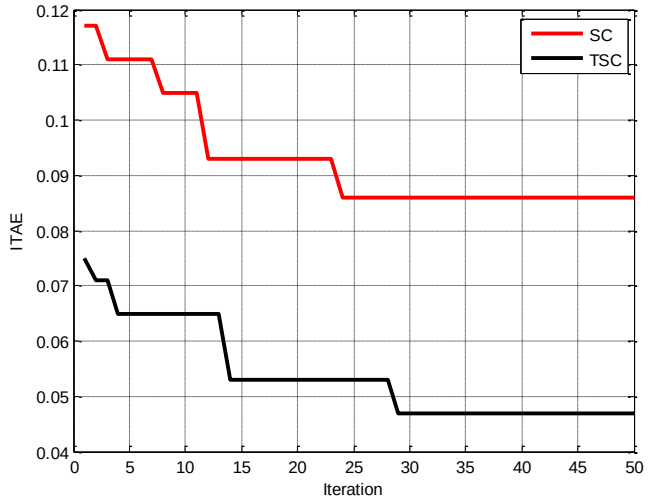

Fig. 3. Convergence of WSA

Fig. 4 and Fig. 5 present the time response of the position of the Magb system to a step input and control signal, respectively. The performance assessment is measured by the following metrics: settling time (t_s), stead state error $(e_{s.s})$, maximum overshoot (Mo), and ITAE. The quantitative of these metrics are recorded in Table III.

It can be seen form Fig. 4 with the help of Table III, that both controllers (TSC and CSC) are effectively able to control the position of the Magb system with zero Mo and zero $e_{s.s}$. However, the TSC achieves better response in terms of tracking to the desired position than the SC where t_s is reduced from 0.4s for the CSC to 0.2s for the TSC. This improvement leads to improve the ITAE index of the TSC by 45.34%. This means, the value ITAE index is declined from the value of 0.086 for the CSC to the value of 0.047 for the TSC. Additionally, the two controllers have free-chattering problem in the control law as seen in Fig. 5. Furthermore, by comparing the performance of the TCS with other nonlinear controller such as sliding mode control (SMC) and backstepping control (BSC), it can be seen that the dynamic response of TSC is better than that of SMC and BSC [12] in terms of reducing t_s and cost function (ITAE) as shown in Table IV.

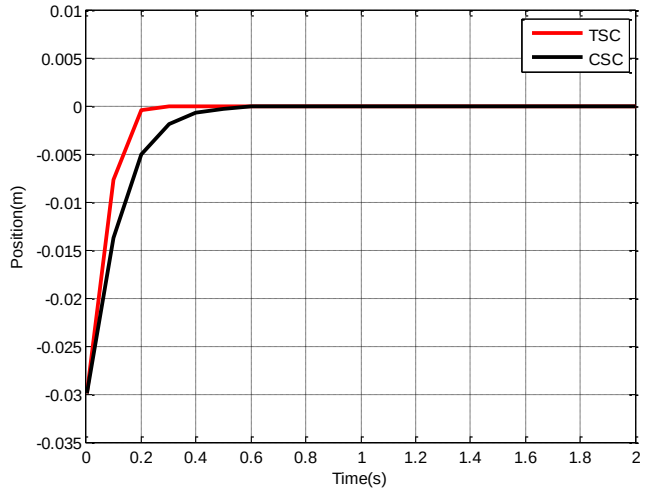

Fig. 4. Response of Magb system's position

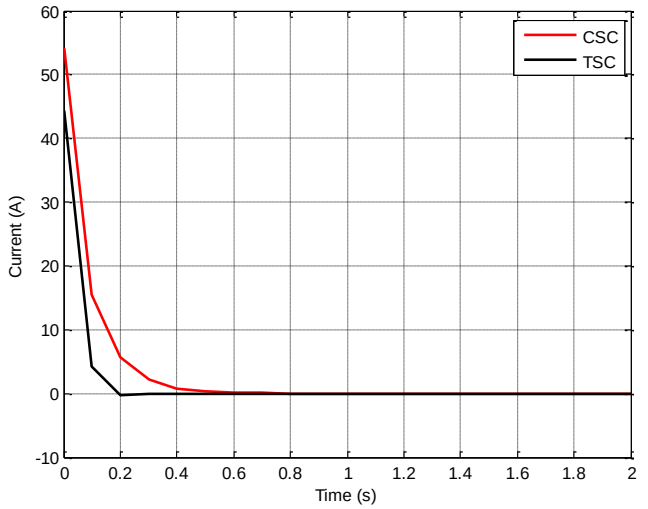

Fig. 5. Control signals of proposed controllers

TABLE III. DYNAMIC PERFORMANCES OF SYSTEM

Controller	$t_s(s)$	$e_{s.s}(rad)$	$Mo(\%)$	ITAE
TSC	0.2	0	0	0.047
SC	0.4	0	0	0.086
Ref[12] SMC	0.3	0	0	0.075
Ref[12] BSC	0.45	0	0	0.107

B. Scenario 2: with Disturbance

In this scenario, an external disturbance was applied to the system after 2 s of the simulation duration. The same settings of TSC and CSC that were obtained in scenario 1 were used to evaluate the performance of the two controllers when the system is subjected to an external disturbance. Fig. 6 depicts the responses of the Magb system under external disturbance. The evaluation of the performance of the controlled system in the disturbance scenario is measured according to recovery time (t_r) and maximum undershoot (Mu). The dynamics response of the two controllers with disturbance is listed in Table IV. It can be observed from the Fig. 6 with the numerical data in the Table IV that the rotor of the bearing is recovery from the disturbance to the predefine position and stayed stable for both controllers. Nevertheless, the Mu value of the TSC is 5% and the time t_r is 0.2 s. this results are better when compared with the 10% Mu and 0.4 s t_r of the SC. Furthermore, by comparing the performance of the TCS with the results of SMC and BSC [12], it can be seen that the disturbance rejection of TSC is better than that of SMC and BSC.

TABLE IV. DYNAMIC PERFORMANCES OF SYSTEM WITH DISTURBANCE

Controller	$t_r(s)$	$Mu(\%)$
TSC	0.2	5%
SC	0.4	10%
SMC Ref[12]	1	13%
BSC Ref [12]	1.5	30%

Under these extensive evaluations of the TSC with CSC, SMC and BSC, the observation is that the TSC's exhibits superior performance to control the Magb as compared to other nonlinear controllers in the context of performance and robustness.

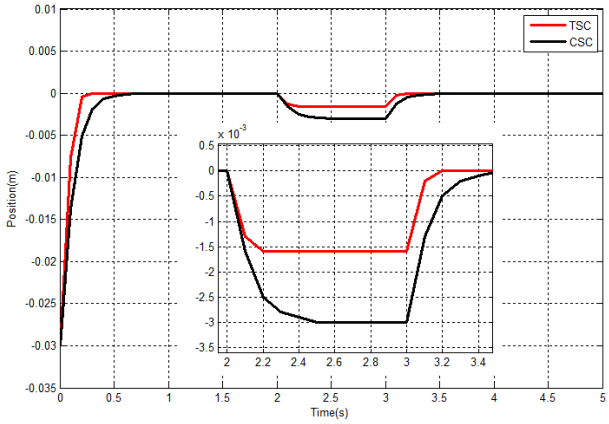

Fig. 6. Response of Magb system's position with disturbance

VI. CONCLUSION

In this paper, terminal synergetic control (TSC) algorithm design for magnetic bearing (Magb) system is presented. The water strider optimizer (WSA) is employed to optimize the control parameters and remove the difficulty of choosing these parameters. Computer simulations based on MATLAB software were made to verify the performance of the proposed control algorithm. The simulation results show that TSC and CSC are able to control the Magb system without overshoot and with zero error steady state. However, the TSC has a good control performance in improving transient response in terms of settling time and reduce the effect of external disturbance in comparing with the classical SC and other state-of-art nonlinear controller such as sliding mode control (SMC) and backstepping control (BSC). For example, the TSC reduce the settling time by 50%, 33.33% and 55.5% as compared to the CSC, SMC, and BSC respectively. Additionally, the ITAE index is reduced by 45.3%, 37.3% and 60% as compared to the CSC, SMC, and BSC respectively. In the context of disturbance resilience, the recovery time of the TSC is reduced by 50%, 80% and 86.6% as compared to the CSC, SMC and BSC. This improvement allows to optimization of the Magb system efficiency. This work could be further improved through the implementation of another controller such as passivity-based control combined with sliding mode control [54] for the Magb system. To handle uncertainties in the system parameters, synergetic-based adaptive control design could be applied [55]-[57]. In the case of the system's states cannot be directly measured, their estimates can be obtained from a state observer [58]-[60].

REFERENCES

[1] X. Wang, Y. Zhang, and P. Gao, "Design and analysis of second-order sliding mode controller for active magnetic bearing," *Energies*, vol. 13, no. 22, p. 5965, 2020.

[2] G. Donati, M. Basso, G.A. Manduzio, M. Mugnaini, T. Pecorella, and C. Camerota, "A convolutional neural network for electrical fault recognition in active magnetic bearing systems," *Sensors*, vol. 23, no. 16, p. 7023, 2023.

[3] Y. Xu, Q. Shen, Y. Zhang, J. Zhou, and C. Jin, "Dynamic modeling of the active magnetic bearing system operating in base motion condition," *IEEE Access*, vol. 8, pp. 166003-166013, 2020.

[4] T. K. Psonis, P. G. Nikolakopoulos, and E. Mitronikas, "Design of a PID controller for a linearized magnetic bearing," *International Journal of Rotating Machinery*, vol. 2015, pp. 1-12, 2015.

[5] W. Bo, G. Haipeng, L. Hao, and Z. Wei, "Particle swarm optimization-based fuzzy PID controller for stable control of active magnetic bearing system," in *Journal of Physics: Conference Series*, vol. 1888, no. 1, p. 012022, 2021.

[6] S. Gupta, J. Laldingliana, S. Debnath, and P. K. Biswas, "Closed loop control of active magnetic bearing using PID controller," in *2018 International Conference on Computing, Power and Communication Technologies (GUCON)*, pp. 686-690, 2018.

[7] S. Yixin, L. Xuan, Z. Zude, C. Youping, and Z. Danhong, "Fuzzy-immune PID control for AMB systems," *Wuhan University Journal of Natural Sciences*, vol. 11, no. 3, pp. 637-641, 2006.

[8] H. Du, Q. Cui, P. Liu, X. Ma, and H. Wang, "PID controller enhanced with artificial bee colony algorithm for active magnetic bearing," *Systems Science & Control Engineering*, vol. 10, no. 1, pp. 686-697, 2022.

[9] R. P. Jastrzębski and R. Pöllänen, "Centralized optimal position control for active magnetic bearings: comparison with decentralized control," *Electrical Engineering*, vol. 91, pp. 101-114, 2009.

[10] L. Y. Chang and H. C. Chen, "Tuning of fractional PID controllers using adaptive genetic algorithm for active magnetic bearing system," *WSEAS Transactions on systems*, vol. 8, no. 1, pp. 158-167, 2009.

[11] T. Yu, Z. Zhang, Y. Li, W. Zhao, and J. Zhang, "Improved active disturbance rejection controller for rotor system of magnetic levitation turbomachinery," *Electronic Research Archive*, vol. 31, no. 3, pp. 1570-1586, 2023.

[12] H. Al-Khazraji, R. M. Naji, and M. K. Khashan, "Optimization of Sliding Mode and Back-Stepping Controllers for AMB Systems Using Gorilla Troops Algorithm," *Journal Européen des Systèmes Automatisés*, vol. 57, no. 2, pp. 417–424, 2024.

[13] H. Al-Khazraji, K. Al-Badri, R. Al-Majeez, and A. J. Humaidi, "Synergetic Control Design Based Sparrow Search Optimization for Tracking Control of Driven-Pendulum System," *Journal of Robotics and Control (JRC)*, vol. 5, no. 5, pp. 1549-1556, 2024.

[14] A. K. Abbas and S. K. Kadhim, "Dynamic Motion Control of Two-Link Robots with Adaptive Synergetic Algorithms," *Journal of Robotics and Control (JRC)*, vol. 5, no. 5, pp. 1536-1548, 2024.

[15] H. Al-Khazraji, K. Albadri, R. Almajeez, and A. J. Humaidi, "Synergetic Control-Based Sea Lion Optimization Approach for Position Tracking Control of Ball and Beam System," *International Journal of Robotics and Control Systems*, vol. 4, no. 4, pp. 1547-1560, 2024.

[16] H. Benbouhenni and N. Bizon, Terminal synergetic control for direct active and reactive powers in asynchronous generator-based dual-rotor wind power systems," *Electronics*, vol. 10, no. 16, p. 1880, 2021.

[17] A. K. Ahmed and H. Al-Khazraji, "Optimal Control Design for Propeller Pendulum Systems Using Gorilla Troops Optimization," *Journal Européen des Systèmes Automatisés*, vol. 56, no. 4, pp. 575-582, 2023.

[18] H. Al-Khazraji, "Optimal Design of a Proportional-Derivative State Feedback Controller Based on Meta-Heuristic Optimization for a Quarter Car Suspension System," *Mathematical Modelling of Engineering Problems*, vol. 9, no. 2, pp. 437-442 2022.

[19] H. Al-Khazraji, C. Cole and W. Guo, "Dynamics analysis of a production-inventory control system with two pipelines feedback," *Kybernetes*, vol. 46, no. 10, pp. 1632-1653, 2017.

[20] R. M. Naji, H. Dulaimi, and H. Al-Khazraji, "An Optimized PID Controller Using Enhanced Bat Algorithm in Drilling Processes," *Journal Européen des Systèmes Automatisés*, vol. 57, no. 3, pp. 767-772, 2024.

[21] M. A. AL-Ali, O. F Lutfy, and H. Al-Khazraj, "Comparative Study of Various Controllers Improved by Swarm Optimization for Nonlinear Active Suspension Systems with Actuator Saturation," *International Journal of Intelligent Engineering & Systems*, vol. 17, no. 4, pp. 879-881, 2024.

[22] Z. N. Mahmood, H. Al-Khazraji, and S. M. Mahdi, "Adaptive control and enhanced algorithm for efficient drilling in composite materials," *Journal Européen des Systèmes Automatisés*, vol. 56, no. 3, pp. 507-512, 2023.

[23] H. Al-Khazraji, C. Cole, and W. Guo, "Analysing the impact of different classical controller strategies on the dynamics performance

of production-inventory systems using state space approach," *Journal of Modelling in Management*, vol. 13, no. 1, pp. 211-235, 2018.

[24] X. S. Yang, "Nature-inspired optimization algorithms: Challenges and open problems," *Journal of Computational Science*, vol. 46, p. 101104, 2020.

[25] N. Mittal, U. Singh, and B. S. Sohi, "Modified grey wolf optimizer for global engineering optimization," *Applied Computational Intelligence and Soft Computing*, vol. 2016, no. 1, p. 7950348, 2016.

[26] A. K. Kar, "Bio inspired computing–a review of algorithms and scope of applications," *Expert Systems with Applications*, vol. 59, pp. 20-32, 2016.

[27] H. Al-Khazraji, S. Khlil, and Z. Alabacy, "Cuckoo search optimization for solving product mix problem," in *IOP Conference Series: Materials Science and Engineering*, vol. 1105, no. 1, p. 012016, 2021.

[28] S. Khlil, H. Al-Khazraji, and Z. Alabacy, "Solving assembly production line balancing problem using greedy heuristic method," in *IOP Conference Series: Materials Science and Engineering*, vol. 745, no. 1, p. 012068, 2020

[29] H. AL-Khazraji, C. Cole, and W. Guo, "Optimization and simulation of dynamic performance of production–inventory systems with multivariable controls," *Mathematics*, vol. 9, no. 568, pp. 1-13, 2021.

[30] F. R Yaseen, M. Q. Kadhim, H. Al-Khazraji, and A. J. Humaidi, "Decentralized Control Design for Heating System in Multi-Zone Buildings Based on Whale Optimization Algorithm," *Journal Européen des Systèmes Automatisés*, vol. 57, no. 4, pp. 981-989, 2024.

[31] E. S. Ghith and F. A. A. Tolba, "Design and optimization of PID controller using various algorithms for micro-robotics system," *Journal of Robotics and Control (JRC)*, vol. 3, no. 3, pp. 244-256, 2022.

[32] H. Al-Khazraji, "Comparative study of whale optimization algorithm and flower pollination algorithm to solve workers assignment problem," *Int. J. Prod. Manag. Eng.*, vol. 10, no. 1, pp. 91–98, 2022.

[33] R. Z. Khaleel, H. Z. Khaleel, A. Al-Hareeri, M. Al-Obaidi, and A. J. Humaidi, "Improved Trajectory Planning of Mobile Robot Based on Pelican Optimization Algorithm," *Journal Européen des Systèmes Automatisés*, vol. 57, no. 4, p. 1005, 2024.

[34] H. Al-Khazraji, S. Khlil, and Z. Alabacy, "Industrial picking and packing problem: Logistic management for products expedition," *Journal of Mechanical Engineering Research and Developments*, vol. 43, no. 2, pp. 74-80, 2020.

[35] B. Bhatt, H. Sharma, K. Arora, G. P. Joshi, and B. Shrestha, "Levy flight-based improved grey wolf optimization: a solution for various engineering problems," *Mathematics*, vol. 11, no. 7, p. 1745, 2023.

[36] W. Aribowo, M. Rohman, F. Baskoro, R. Harimurti, Y. Yamasari, and W. Yustanti, "A Novel Hybrid Prairie Dog Optimization Algorithm-Marine Predator Algorithm for Tuning Parameters Power System Stabilizer," *Journal of Robotics and Control (JRC)*, vol. 4, no. 5, pp. 686-695, 2023.

[37] H. Al-Khazraji, S. Khlil, and Z. Alabacy, "Solving mixed-model assembly lines using a hybrid of ant colony optimization and greedy algorithm," *Engineering and Technology Journal*, vol. 40, no. 1, pp. 172-180, 2022.

[38] A. K. Ahmed, H. Al-Khazraji, and S. M. Raafa, "Optimized PI-PD Control for Varying Time Delay Systems Based on Modified Smith Predictor," *International Journal of Intelligent Engineering & Systems*, vol. 17, no. 1, pp. 331-342, 2024.

[39] H. A. Azzawi, N. M. Ameen, and S. A. Gitaffa, "Comparative Performance Evaluation of Swarm Intelligence-Based FOPID Controllers for PMSM Speed Control," *Journal Européen des Systèmes Automatisés*, vol. 56, no. 3, 2023.

[40] M. A. Al-Ali, O. F. Lutfy, and H. Al-Khazraj, "Investigation of Optimal Controllers on Dynamics Performance of Nonlinear Active Suspension Systems with Actuator Saturation," *Journal of Robotics and Control (JRC)*, vol. 5, no. 4, pp. 1041-1049, 2024.

[41] H. Al-Khazraji, C. Cole, and W. Guo, "Multi-objective particle swarm optimisation approach for production-inventory control systems," *Journal of Modelling in Management*, vol. 13, no. 4, pp. 1037-1056, pp.879-887, 2018.

[42] M. A. Hasan, A. A. Oglah, and M. J. Marie, "Optimal FOPI-FOPD controller design for rotary inverted pendulum system using grey wolves' optimization technique," *TELKOMNIKA (Telecommunication Computing Electronics and Control)*, vol. 21, no. 3, pp. 657-666, 2023.

[43] S. A. Eissa, S. W. Shneen, and E. H. Ali, "Flower Pollination Algorithm to Tune PID Controller of TCP/AQM Wireless Networks," *Journal of Robotics and Control (JRC)*, vol. 4, no. 2, pp. 149-156, 2023.

[44] H. Al-Khazraji, W. Guo, and A. J. Humaidi, "Improved cuckoo search optimization for production inventory control systems," *Serbian Journal of Electrical Engineering*, vol. 21, no. 2, pp. 187-200, 2024.

[45] R. A. Kadhim, M. Q. Kadhim, H. Al-Khazraji, and A. J. Humaidi, "Bee Algorithm Based Control Design for Two-links Robot Arm Systems," *IIUM Engineering Journal*, vol. 25, no. 2, pp. 367-380, 2024.

[46] M. E. Sadiq, A. J. Humaidi, S. K. Kadhim, A. Al Mhdawi, A. Alkhayyat, and I. K. Ibraheem, "Optimal sliding mode control of single arm PAM-actuated manipulator," in *2021 IEEE 11th International Conference on System Engineering and Technology (ICSET)*, pp. 84-89, 2021.

[47] A. Kaveh and A. D. Eslamlou, "Water strider algorithm: A new metaheuristic and applications," in *Structures*, vol. 25, pp. 520-541, 2020.

[48] X. Zhang, J. Zhao, Q. Zhu, N. Chen, M. Zhang, and Q. Pan, "Bioinspired aquatic microrobot capable of walking on water surface like a water strider," *ACS applied materials & interfaces*, vol. 3, no. 7, pp. 2630-2636, 2011.

[49] D. L. Hu and J. W. Bush, "The hydrodynamics of water-walking arthropods," *Journal of Fluid Mechanics*, vol. 644, pp. 5-33, 2010.

[50] R. S. Wilcox, "Ripple communication in aquatic and semiaquatic insects," *Ecoscience*, vol. 2, no. 2, pp. 109-115, 1995.

[51] D. D. Williams and B. W. Feltmate. *Aquatic insects.* Cab International, 1992.

[52] A. Lipowski, D. Lipowska, "Roulette-wheel selection via stochastic acceptance," *Physica A*, vol. 391, no. 6, pp. 2193–2196, 2012.

[53] Z. N. Mahmood, H. Al-Khazraji, and S. M. Mahdi, "PID-Based Enhanced Flower Pollination Algorithm Controller for Drilling Process in a Composite Material," *Annales de Chimie Science des Matériaux*, vol. 47, no. 2, pp. 91-96, 2023.

[54] M. N. Huynh, H. N. Duong, and V. H. Nguyen, "A passivity-based control combined with sliding mode control for a DC-DC boost power converter," *Journal of Robotics and Control (JRC)*, vol. 4, no. 6, pp. 780-790, 2023.

[55] S. M. Mahdi, N. Q. Yousif, A. A. Oglah, M. E. Sadiq, A. J. Humaidi, and A. T. Azar, "Adaptive synergetic motion control for wearable knee-assistive system: a rehabilitation of disabled patients," *Actuators*, vol. 11, no. 7, p. 176, 2022.

[56] A. F. Mutlak and A. J. Humaidi, "Adaptive synergetic control for electronic throttle valve system," *International Review of Applied Sciences and Engineering*, vol. 15, no. 2, pp. 211-220, 2024.

[57] A. J. Humaidi, I. K. Ibraheem, A. T. Azar, and M. E. Sadiq, "A new adaptive synergetic control designs for single link robot arm actuated by pneumatic muscles," *Entropy*, vol. 22, no. 7, p. 723, 2020.

[58] Z. Zhang, J. Cheng, and Y. Guo, "PD-based optimal ADRC with improved linear extended state observer," *Entropy*, vol. 23, no. 7, p. 888, 2021.

[59] N. S. Mahmood, A. J. Humaidi, R. S. Al-Azzawi, and A. Al-Jodah, "Extended state observer design for uncertainty estimation in electronic throttle valve system," *International Review of Applied Sciences and Engineering*, vol. 15, no. 1, pp. 107-115, 2024.

[60] N. A. Alawad, A. J. Humaidi, A. S. M. Al-Obaidi, and A. S. Alaraji, "Active disturbance rejection control of wearable lower-limb system based on reduced ESO," *Indonesian Journal of Science and Technology*, vol. 7, no. 2, pp. 203-218, 2022.